

Regular paper

Acetylated Xylan Degradation by Glycoside Hydrolase Family 10 and 11 Xylanases from the White-rot Fungus *Phanerochaete chrysosporium*

(Received December 27, 2021; Accepted February 28, 2022)

(J-STAGE Advance Published Date: March 5, 2022)

Keisuke Kojima,¹ Naoki Sunagawa,¹ Yoshihisa Yoshimi,² Theodora Tryfona,² Masahiro Samejima,^{1,3} Paul Dupree,² and Kiyohiko Igarashi^{1,†}

¹ Department of Biomaterial Sciences, The University of Tokyo
(1-1-1 Yayoi, Bunkyo-ku, Tokyo 113-8657, Japan)

² Department of Biochemistry, University of Cambridge
(Cambridge, Cambridgeshire, CB2 1QW, United Kingdom)

³ Faculty of Engineering, Shinshu University
(4-17-1 Wakasato, Nagano 380-8533, Japan)

Abstract: Endo-type xylanases are key enzymes in microbial xylanolytic systems, and xylanases belonging to glycoside hydrolase (GH) families 10 or 11 are the major enzymes degrading xylan in nature. These enzymes have typically been characterized using xylan prepared by alkaline extraction, which removes acetyl sidechains from the substrate, and thus the effect of acetyl groups on xylan degradation remains unclear. Here, we compare the ability of GH10 and 11 xylanases, *PcXyn10A* and *PcXyn11B*, from the white-rot basidiomycete *Phanerochaete chrysosporium* to degrade acetylated and deacetylated xylan from various plants. Product quantification revealed that *PcXyn10A* effectively degraded both acetylated xylan extracted from *Arabidopsis thaliana* and the deacetylated xylan obtained by alkaline treatment, generating xylooligosaccharides. In contrast, *PcXyn11B* showed limited activity towards acetyl xylan, but showed significantly increased activity after deacetylation of the xylan. Polysaccharide analysis using carbohydrate gel electrophoresis showed that *PcXyn11B* generated a broad range of products from native acetylated xylans extracted from birch wood and rice straw, including large residual xylooligosaccharides, while non-acetylated xylan from Japanese cedar was readily degraded into xylooligosaccharides. These results suggest that the degradability of native xylan by GH11 xylanases is highly dependent on the extent of acetyl group substitution. Analysis of 31 fungal genomes in the Carbohydrate-Active enZymes database indicated that the presence of GH11 xylanases is correlated to that of carbohydrate esterase (CE) family 1 acetyl xylan esterases (AXEs), while this is not the case for GH10 xylanases. These findings may imply co-evolution of GH11 xylanases and CE1 AXEs.

Key words: xylanase, glycoside hydrolase, acetylated xylan, *Phanerochaete chrysosporium*, biomass utilization

INTRODUCTION

Plant cell walls are composed of three main components, i.e., cellulose, hemicellulose and lignin, and enzymatic

saccharification is a mild and effective way to utilize cellulose and hemicellulose as a source of biofuel and bio-based chemicals that can replace fossil resources. Recently, it was shown that the degradation of hemicellulose is the bottleneck in enzymatic saccharification of plant biomass,¹⁾ and thus degradation of hemicellulose is as important as that of cellulose. In plant cell walls, hemicelluloses interact strongly with other components. For instance, xylan, a common hemicellulose of terrestrial plants, can be on the surface of cellulose^{2,3)} and can also be chemically linked to lignin to form lignin-carbohydrate complexes.^{4,5)}

The main chain of xylan consists of β -1,4-linked xylose residues, whereas the side chains, such as glucuronic acid (GlcA), arabinofuranose (Araf) and acetyl groups (Ac), differ among different plant species. Acetylation in hardwood secondary cell walls is largely on alternate xylose residues and can substitute O2 and/or O3 of xylose residues with a degree of acetylation over 0.5.⁶⁾ In gymnosperm, softwoods,

[†]Corresponding author (Tel. +81-5841-5255, E-mail: aquarius@mail.ecc.u-tokyo.ac.jp, ORCID ID 0000-0001-5152-7177).

Abbreviations: Ac, acetyl group; ANTS, 8-aminonaphthalene-1,3,6-trisulfonic acid; Araf, arabinofuranose; AXE, acetyl xylan esterase; BCA, bichinchonic acid; CjGH10, GH10 xylanase from *Cellvibrio japonicus*; DMSO, dimethyl sulfoxide; DP, degree of polymerization; DW, distilled water; GH, glycoside hydrolase; GlcA, glucuronic acid; MW, molecular weight; NpGH11, GH11 xylanase from *Neocallimastix patriciarum*; PACE, polysaccharide analysis using carbohydrate gel electrophoresis; *PcXyn10A*, GH10 xylanase from *Phanerochaete chrysosporium*; *PcXyn11B*, GH11 xylanase from *P. chrysosporium*; X₂, xylobiose; X₃, xylotriose; X₄, xylo-tetraose; X₅, xylopentaose; X₆, xylohexaose.

This is an open-access paper distributed under the terms of the Creative Commons Attribution Non-Commercial (by-nc) License (CC-BY-NC4.0: <https://creativecommons.org/licenses/by-nc/4.0/>).

xylan is not acetylated, while there are moderate levels of acetylation in grasses.⁷⁾ In nature, xylan is degraded by a series of enzymes produced by fungi and bacteria.⁸⁾⁹⁾ Main chain degradation is performed by endo-xylanases (Xyn, EC 3.2.1.8), which can degrade xylan polymer into xylooligosaccharides, and then β -xylosidase (EC 3.2.1.37) produces xylose monomer from the xylooligosaccharides, with an aid of accessory enzymes. GlcA, Araf, and Ac are removed by xylan α -1,2-glucuronosidase (EC 3.2.1.131), α -L-arabinofuranosidase (EC 3.2.1.55), and acetyl xylan esterase (AXE, EC 3.2.1.72), respectively.

Most of fungal xylanases, the key enzymes of the xylan degradation system, are classified into glycoside hydrolase (GH) families 10, 11, and 30 in the Carbohydrate-Active enZymes (CAZy) database (<http://www.cazy.org/>).¹⁰⁾ GH10 and 11 xylanases, the major enzymes among wood-decay fungi,¹¹⁾ are reported to show no distinct substrate preferences, i.e., both enzymes are capable of degrading various xylooligosaccharides and non-acetylated xylan, based on their reaction properties and crystal structures.¹²⁾¹³⁾¹⁴⁾¹⁵⁾¹⁶⁾ However, although those substrates lack acetyl groups, native xylans from plants other than gymnosperm are modified with acetyl groups, and the products of degradation of acetylated xylan by GH10 and 11 xylanases are quite diverse.⁹⁾ Thus, the substrate specificity of xylanases towards acetylated xylan remains unclear. The aim of this work was to investigate the substrate preferences of GH10 and 11 xylanases from the basidiomycete *Phanerochaete chrysosporium*¹⁷⁾ (*PcXyn10A* and *PcXyn11B*) by means of time course experiments and analysis of the final products generated from native acetylated xylan, deacetylated xylan obtained by alkaline treatment and non-acetylated xylan.

MATERIALS AND METHODS

Cloning. *P. chrysosporium* strain K-3 was grown on Kremer and Wood medium¹⁸⁾ containing 2 % Avicel (Sigma-Aldrich, MA, USA) as the sole carbon source. Total RNA was extracted from approximately 100 mg of frozen mycelial powder using RNeasy (QIAGEN, Limburg, Netherlands), and mRNA was purified using Oligo dT Latex (Takara Bio Inc., Shiga, Japan), as per the instructions. cDNA from mRNA was synthesized using a GeneRacer kit (Invitrogen, Waltham, MA, USA). The primers for amplification from cDNA were designed based on the genomic sequences of *P. chrysosporium* as shown in Table S1 (see J. Appl. Glycosci. Web site). To determine and obtain the full-length sequences of *pcxyn10a*, the primers FW_PcXyn10A_5'UTR2 and RV_PcXyn10A_3'UTR2 were used. For *pcxyn11b*, FW_PcXyn11B_5'UTR and RV_PcXyn11B_3'UTR were used. All PCR products were cloned using a Zero Blunt TOPO PCR Cloning kit for Sequencing (Thermo Fisher Science Inc., Waltham, MA, USA). The amino acid sequences of *PcXyn10A* and *PcXyn11B* were analyzed by SignalP 5.0¹⁹⁾ and Pfam 31.0²⁰⁾ to identify signal peptides and domain structures, respectively. pPICZ α plasmid with Ste13 cleavage sites removed and *pcxyn10a* or *pcxyn11b* were fused using an In-Fusion HD cloning Kit (Takara Bio Inc.). Each sequence was located between Kex2 and Xba I sites in the pPICZ α plasmid. After transformation of the methylotrophic *Pichia pastoris* strain KM71H by electroporation,

transformants were selected using Zeocin according to the manual.

Enzyme preparations. Recombinant proteins were obtained by using a 5-L jar fermenter (TSC-M5L; Takasugi Seisakusho, Tokyo, Japan) with methanol feed according to the reported method.²¹⁾²²⁾ After protein production was finished, each medium was collected by centrifugation at $5,000 \times G$ for 30 min.

The collected medium was passed through a 100 kDa filter and concentrated using a 10 kDa filter (Millipore, Corporation, Billerica, MA, USA). The concentrate was purified on a hydrophobic interaction column (TOYOPEARL Phenyl 650M, Tosoh Corporation, Tokyo, Japan). After equilibration with 50 mM sodium acetate buffer (pH 5.0) containing 1 M ammonium sulfate (FUJIFILM Wako Pure Chemical Co., Osaka, Japan), enzymes were eluted with 50 mM sodium acetate buffer (pH 5.0). An anion-exchange column (TOYOPEARL 650S, Tosoh Corporation) was used for further purification. After equilibration with 50 mM Tris-HCl buffer (pH 7.0), the enzymes were eluted with 50 mM Tris-HCl buffer (pH 7.0) containing 1 M NaCl. To confirm purity, 12 % SDS-PAGE was performed.

GH10 xylanase from *Cellvibrio japonicus* (*CjGH10*)²³⁾ was a kind gift from Professor Harry Gilbert (York University) and GH11 xylanase from *Neocallimastix patriciarum* (*NpGH11*)¹⁵⁾ was purchased from Megazyme (Wicklow, Ireland).

Crude protein was quantified using the Bradford Protein Assay (Bio-Rad Laboratories, Inc., Hercules, CA, USA) with bovine serum albumin as a standard. Purified enzymes were quantified with a NanoDrop2000 (Thermo Fisher Scientific Inc.).

Preparation of native xylans from various plants. Acetylated xylan from *Arabidopsis thaliana* was extracted based on the method reported by Busse-Wicher *et al.*⁶⁾ Approximately 100 mg of alcohol-insoluble residue from stems of *A. thaliana*, prepared as previously described,²⁴⁾ was depectinated in 0.5 (w/v) % ammonium oxalate at 85 °C for 2 h. The sample was then washed with water and delignified in 11 % peracetic acid at 85 °C for 30 min. Finally, acetylated xylan was extracted from holocellulose with dimethyl sulfoxide (DMSO), and the solvent was changed to distilled water (DW) using a PD-10 column (GE Healthcare, Chicago, IL, USA). For analysis of the sugar content, TFA hydrolysis of this acetylated xylan and high-pressure ion chromatography using Dionex (Dionex Corporation, Sunnyvale, CA, USA) were conducted.

Native xylans were also extracted from birch wood, Japanese cedar, and rice straw. Wood blocks and rice straw were dried, milled and meshed as described previously.¹⁾ Samples were depectinated as described above and delignified according to Kludiz.²⁵⁾²⁶⁾ One gram of powder sample, 0.8 g of NaClO₂ and 150 mg of acetic acid (FUJIFILM Wako Pure Chemical Co.) were mixed with 11 mL of DW and incubated at 37 °C for 40 h. Acetylated xylans were extracted from birch wood and rice straw with DMSO, and non-acetylated xylan was extracted from Japanese cedar with 4 M KOH. After extraction, the solvents were replaced with DW as described above.

To estimate the ratio of xylan components, ¹H-NMR spectra were acquired at 20 °C on a 500 MHz spectrometer

(JNM-ECA500II, JEOL Ltd., Tokyo, Japan). For NMR, non-acetylated xylan from Japanese cedar was purified by adding saturated Ba(OH)₂ (FUJIFILM Wako Pure Chemical Co.) solution to precipitate mannan. Approximately 20 mg of each substrate was dissolved in 1 mL of D₂O (Sigma-Aldrich) and centrifuged to remove solids. The results were analyzed by means of delta software (version 6.0.0, JEOL Ltd.). The ¹H NMR assignments were conducted by comparison with reported NMR spectral data for acetylated xyans from dicots,²⁷⁾²⁸⁾²⁹⁾ acetylated xyans from grasses⁷⁾³⁰⁾ and non-acetylated xylan from softwood.³¹⁾ The peak of xylose residue without side chain (Free Xyl: 4.33 ppm), those of GlcA-substituted xylose residue (GlcA-Xyl: 4.96 and 5.15 ppm), those of acetylated xylose residue (Ac-Xyl: 4.42, 4.55, 4.96, and 5.03 ppm), that of Ara_f-substituted xylose residue (Ara_f-Xyl: 5.25 ppm) were assigned and integrated. The ratio of xylan components was estimated from the peak area ratios (Table 1).

Time course study. The increase in the amount of reducing ends was measured by means of the bicinchoninic acid (BCA, Tokyo Chemical Industry Co., Ltd., Tokyo, Japan) method³²⁾ with few modifications. The reaction solution consisted of 4 nM purified enzyme, 1.67 μM acetylated xylan from *A. thaliana*, and 50 mM ammonium acetate buffer (pH 5.0). The reaction was stopped at 0, 5, 10, 30, and 60 min by adding alkali solution in BCA methods. The ratio of each sample, solution A (5.65 mM BCA, 512 mM and 288 mM NaHCO₃) and solution B (7.82 mM CuSO₄·5H₂O and 12.0 mM L-serine) was 1: 2: 2. Those mixed samples were heated at 80 °C for 30 min and cooled on ice. Finally, the absorbance at 560 nm was determined and the concentration of produced reducing ends was calculated based on a xylose standard curve. Results were fit to the following first-order equation using R (version 3.6.3),

$$y = S(1 - e^{-t/\tau})$$

where y and t are the concentration of released reducing ends (μM) and the reaction time (h), respectively, S is the concentration of degradable regions of each substrate (μM) by different xylanases. τ is the time constant (h).

Alkaline treatment of the same acetylated xylan was conducted for deacetylation to prepare deacetylated xylan polymer at the same concentration as the acetylated xylan polymer. First, 4 M NaOH was added to acetylated xylan solution and the mixture was incubated at room temperature for 20 min. Then, 1 M HCl was added for neutralization. The ratio of acetylated xylan solution, NaOH and HCl was 200: 5: 20.

Polysaccharide analysis using carbohydrate gel electrophoresis. For analysis of the final products after digestion of acetylated xylan from *A. thaliana*, polysaccharide analysis using carbohydrate gel electrophoresis (PACE)³³⁾ with 10 w/v % polyacrylamide gels was adopted. Gels were prepared as described by Bromley *et al.*³⁴⁾ with modifications in the composition of gels. One 10 w/v % polyacrylamide gel consisted of 20.4 mL of DW, 3 mL of 1 M tris(hydroxymethyl) aminomethane-base borate (pH 8.2), 8.4 mL of 40 % polyacrylamide (29:1; acrylamide/bis), 24 μL of *N, N, N', N'*-tetramethylethylenediamine and 180 μL of 10 % ammonium persulfate. The reaction solution was the same as used for the time course study and was incubated at 30 °C for 24 h. After digestion, samples were dried using a Speed-Vac (Thermo Fisher Scientific Inc.) and labelled overnight with 8-aminonaphthalene-1,3,6-trisulfonic acid (ANTS) as described by Bromley *et al.*³⁴⁾ ANTS-Labelled samples were dried using a Speed-Vac and resuspended in 3 M urea as PACE samples. Standards, a mixture of xylooligosaccharides (Megazyme), were also labelled. Electrophoresis of *A. thaliana* samples was conducted using a Hofer SE660 (Hofer, Inc., Holliston, MA, USA) at 1,000 V for 45 min. Visualization of PACE gels was carried as described by Bromley *et al.*³⁴⁾

For comparison of the degradation of various xyans, large custom glass plates (160 mm width and 300 mm height) and equipment for 10 % PACE gels were obtained from Nihon Eido Corp. (Tokyo, Japan). Composition of the gel was the same as above. Electrophoresis was conducted at 1,000 V for 1 h. PACE gels were visualized in a box covered with aluminum foil, using an LED lighting device (Optocode Corp., Tokyo, Japan) emitting at 365 nm. Image J (version 1.53) was used for analysis of bands intensities.

Correlation analysis between xylanases and AXEs. The correlation coefficients, r , between the numbers of enzymes were calculated as the following equation:

$$r = \frac{\text{cov}(x, y)}{\sigma_x \times \sigma_y}$$

where $\text{cov}(x, y)$, σ_x , and σ_y mean the covariance between x and y , the standard deviation of x and that of y . x and y were the numbers of each enzymes based on previous research.³⁵⁾ For the calculation of those between the existence of enzymes, the numbers were standardized: absence is zero and existence is one.

Table 1. Ratios of xylan components.

Xylan components	Free Xyl (%)	GlcA-Xyl (%)	Ac-Xyl (%)	Ara _f -Xyl (%)
Acetylated xylan from <i>Arabidopsis thaliana</i> ⁶⁾³⁴⁾	34.7 ⁶⁾³⁴⁾	12.1 ³⁴⁾	53.2 ⁶⁾	n.d.
Acetylated xylan from birch wood	45.5 ± 1.2	6.6 ± 0.9	51.1 ± 0.8	n.d.
Acetylated xylan from rice straw	64.5 ± 0.7	0.8 ± 0.1	25.9 ± 0.8	8.7 ± 0.3
Non-acetylated xylan from Japanese cedar	74.8 ± 0.4	17.4 ± 0.2	n.d.	7.8 ± 0.6

The ratio of components of acetylated xylan from *A. thaliana* was taken from the previous reports.⁶⁾³⁴⁾ Based on NMR spectra data for acetylated xyans from dicots,²⁷⁾²⁸⁾²⁹⁾ acetylated xyans from grasses,⁷⁾³⁰⁾ and non-acetylated xylan from softwood,³¹⁾ the peaks were assigned and the ratio of xylan components was estimated from the peak areas. Free Xyl means free xylose residue. GlcA-Xyl, Ac-Xyl, and Ara_f-Xyl mean GlcA-substituted xylose residue, acetylated xylose residue, and Ara_f-substituted xylose residue. n.d. means not detected in this study. Since xylose residues doubly substituted with GlcA and Ac are counted twice, the total is not 100 %.

RESULTS AND DISCUSSION

Cloning and preparation of *PcXyn10A* and *PcXyn11B*.

P. chrysosporium has 6 genes encoding GH10 xylanase and one gene encoding GH11 xylanase.³⁵⁾ Previous reports confirmed that *P. chrysosporium* secretes two GH10 xylanases, *PcXyn10A* and *PcXyn10C*, during culture using only cellulose or cellulose and xylan as carbon resources and that *PcXyn10A* is more constantly expressed than *PcXyn10C*. Therefore, *PcXyn10A* was selected as the representative GH10 xylanase for *P. chrysosporium* in this paper. Cloning of *pcxyn10a* and *pcxyn11b* was successful (Fig. S1; see J. Appl. Glycosci. Web site). *PcXyn10A* and *PcXyn11B* consisted of 389 and 271 amino acids, respectively, and lacked any signal peptide according to SignalP 5.0¹⁹⁾ (Fig. 1). The amino acid sequences were analyzed by HMMER,³⁶⁾ which indicated the presence of a CBM1 domain at the N-terminal and C-terminal ends of *PcXyn10A* and *PcXyn11B*, respectively.

Recombinant *PcXyn10A* and *PcXyn11B* were produced in a jar-fermenter and purified by ultrafiltration and column chromatography. Purity was examined by SDS-PAGE, as shown in Fig. S2 (see J. Appl. Glycosci. Web site), and the purest samples were used for activity testing. Since both proteins contain CBM1 and a linker, the molecular weights are higher than those of the catalytic domain alone. The theoretical molecular weight of *PcXyn10A* is 42,000 and that of *PcXyn11B* is 29,000, whereas the observed values were around 45,000 and 37,000, respectively, in SDS-PAGE. Larger molecular weight of *PcXyn11B* in appearance is consistent with previous results³⁷⁾³⁸⁾ and the large difference between of the two values for *PcXyn11B* is due to glycosylation.

Analysis of the average DP after digestion of acetylated xylan.

The results of digestion of acetylated xylan extracted from *A. thaliana*, in which more than half of the xylose residues are acetylated⁶⁾ (Table 1), is shown in Fig. 2. To compare xylanases from *P. chrysosporium* and well-characterized xylanases, *CjGH10* and *NpGH11* without CBMs were also tested, because *CjGH10* and *NpGH11* were known as

efficient enzymes in GH10 and GH11 xylanases, as additive enzyme to commercial enzymes cocktails for biomass saccharification in the previous report.¹⁾ GH10 xylanases degrade even this densely acetylated xylan into oligosaccharides. Although the τ -values, the time constant, of *PcXyn10A* (0.21 ± 0.02 h) and *CjGH10* (0.12 ± 0.03 h) were somewhat different, the *S*-values, the concentration of degradable regions of the substrate, were similar at 28.0 ± 0.9 and 24.6 ± 1.6 μM , respectively, indicating that both enzymes have similar ability to degrade acetylated xylan (Table 2). Based on the *S*-values, the average DP after reaction was estimated as 9.6 and 11 for *PcXyn10A* and *CjGH10*, respectively. Since the DP of xylan polymer is approximately 150,³⁹⁾ GH10 xylanases cleaved one molecule of acetylated xylan approximately 14 times. After removal of acetyl groups by alkaline treatment, the *S*-values of *PcXyn10A* and *CjGH10* were 47.3 ± 1.2 and 37.4 ± 1.2 μM , respectively, being 1.7 and 1.5 times larger than the values for acetylated xylan. Compared among GH10 xylanases, *CjGH10* showed the smaller values of τ and *S*, suggesting that *CjGH10* can bind substrates more selectively than *PcXyn10A*.

In contrast, GH11 xylanases attacked acetylated xylan from *A. thaliana* much less effectively than did GH10 xylanases, and the *S*-values were 5.2 ± 0.8 μM for *PcXyn11B* and 7.8 ± 0.2 μM for *NpGH11*. The average DPs after digestion were 45 and 32, respectively, indicating that only 3.3 and 4.7 cleavages occurred per acetylated xylan molecule. However, after deacetylation, the *S*-values of *PcXyn11B* and *NpGH11* were 38.0 ± 2.2 and 32.6 ± 0.4 μM , respectively, being 7.3 and 4.2 times higher than those for acetylated xylan. Comparing all xylanases tested, *NpGH11* showed the smallest value of τ for deacetylated xylan, suggesting that *NpGH11* may have evolved to act specifically on deacetylated xylan.

It was reported that acetylation contributes to the resistance of xylan to enzymatic degradation,⁴⁰⁾ and our results show that acetylation has a greater negative effect on GH11 xylanases than on GH10 xylanases. As shown in Table 1, since half of xylose residues are acetylated in *A. thaliana* xylan, the probability of three connected free xylose will appear in every 8 residues. However, in the present results, GH11 xylanases, which require three free xylose

>*PcXyn10A*

QSPVWGQCGGIGWTGPTTCTAGNVCQEYSAYYSQCI PASQATSVTSVSTAPNPPPTSHTSTSSAPSGASTSTAKL
NTLAKAKGKLYFGTATDNGELSDTAYTAI LDDNTMFGQITPANSMKWDATEPQQGQFTFSGGDQIANLAKSNGML
LRGHNCVWYNQLPSVWSNGKFTAAQLTSIIQNHCSTLVTHYKGQVYAWDVVNEPFNDGSRWTDVDFYNTLGTSYV
QIALEAARAADPDAKLYINEYNI EYAGAKATSLNLVTKLAASVPLDGIGFQSHFIVGQVPTGLQSQLTTFAAQ
GVEVAITELDIRMTLPSTPALLAQQKTDYSNVIKACASVEACVGVTVWDWTDKYSWVPNTFSGQGAACPWDQNFV
RKPAYDGLAIGFGN

>*PcXyn11B*

FPPFEFHNGTHVFPRQSTPAGTGTNNGFFYSFWTDGGGVSVTYNNGPAGEYSVTWSNADNFVAGKGNPQSAQAISF
TANYQPNGNSYLSVYGWSTNPLVEYYILEDFTYNPVAVSLTHKGTLSGDGATYDVYEGTRVNEPSIQGTATFNQY
WSIRSSKRSSGTVTTANHF AAWKQLGLPLGTFNYQIVATEGYQSSGSSSTVTVNPAGGVTSPTAPTGPSSVSTTPS
GPSSSPSPVGS CAALYQGCGGQGTGPTCCSSGTCKFSNNWYSQCL

Fig. 1. Amino acid sequences of the xylanases.

PcXyn10A consists of CBM1 (orange) and the GH10 catalytic domain (blue), whereas *PcXyn11B* consists of the GH11 catalytic domain (blue) and CBM1 (orange). The red residues are motifs for binding cellulose. CBM1 from *PcXyn10A* has a WYY motif while that of *PcXyn11B* has a YWY motif.

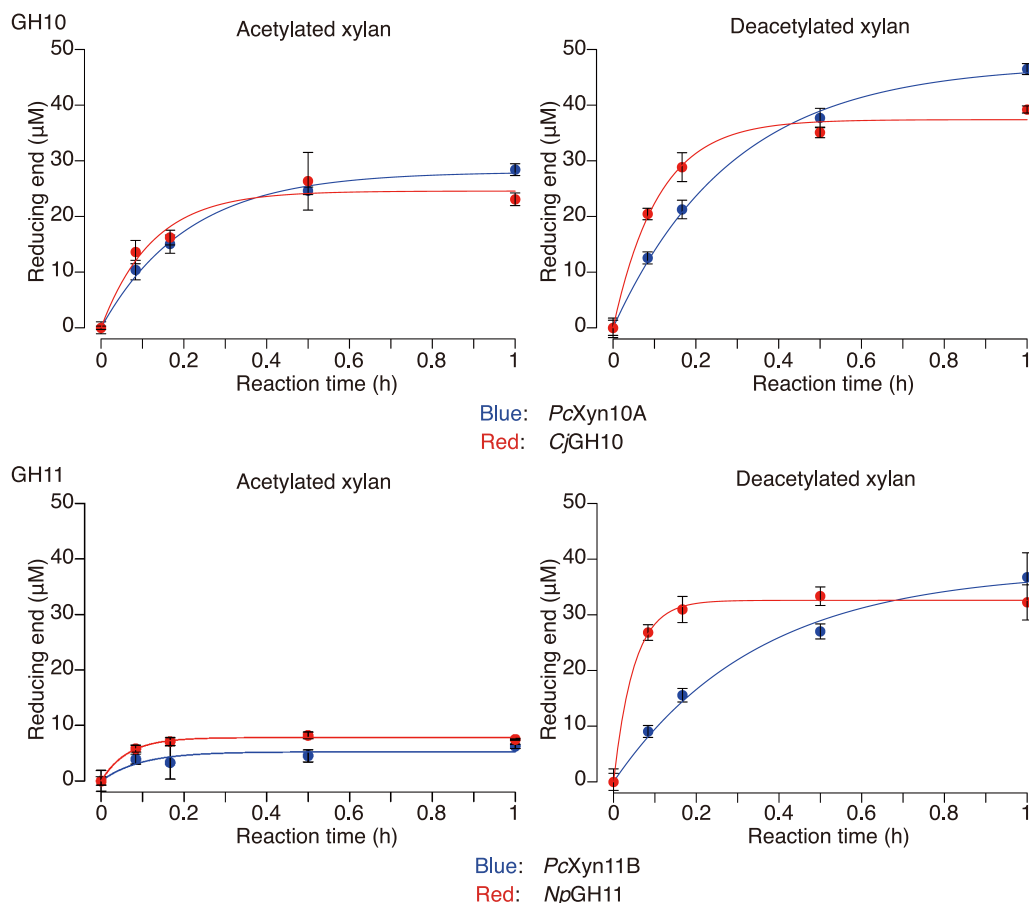


Fig. 2. Time course study of digestion of acetylated xylan and deacetylated xylan.

Reducing-ends during the reaction were measured by the BCA method with few modifications. The reaction solution consisted of 4 nM purified enzyme, 1.67 μ M acetylated xylan from *A. thaliana*, and 50 mM ammonium acetate buffer (pH 5.0). The same amount of DMSO-extracted xylan was treated with alkali for deacetylation using 4 M NaOH for 20 min and then neutralized by adding 1 M HCl. The ratio of xylan solution, 4 M NaOH and 1 M HCl solution was 200:5:20. Curve fitting was performed as described in Materials and Methods section.

Table 2. S and τ values and final average DP from time course study.

Enzyme	Substrate	S (μ M)	τ (h)	Average DP
<i>PcXyn10A</i>	Acetylated xylan	28.0 \pm 0.9	0.21 \pm 0.02	9.6
	Deacetylated xylan	47.3 \pm 1.2	0.29 \pm 0.02	5.8
<i>CjGH10</i>	Acetylated xylan	24.6 \pm 1.6	0.12 \pm 0.03	11
	Deacetylated xylan	37.4 \pm 1.2	0.11 \pm 0.01	7.3
<i>PcXyn11B</i>	Acetylated xylan	5.2 \pm 0.8	0.09 \pm 0.05	45
	Deacetylated xylan	38.0 \pm 2.2	0.34 \pm 0.05	7.2
<i>NpGH11</i>	Acetylated xylan	7.8 \pm 0.2	0.06 \pm 0.01	32
	Deacetylated xylan	32.6 \pm 0.4	0.05 \pm 0.01	8.3

Values of S and τ were determined based on fitting curves for first-order reaction, as shown in Fig. 2. The average DP after reaction was calculated from the S value.

residues,¹⁶⁾ showed less activity than expected, indicating the side chain of acetylated xylan from *A. thaliana* should be regular, which is unfavorable to GH11 activity. Moreover, assuming that the acetyl group modification is every other xylose residue, the degradation of GH10 xylanases did not complete, suggesting that the position of the acetyl group substitutions is important for GH10 to accommodate acetylated xylan. Further analysis of crystal structures with acetylated xylan is necessary to reveal the details.

Analysis of final products by PACE.

A time course study revealed that longer xylooligosaccharides remained undegraded even after prolonged incubation, especially with GH11 xylanases, and the distribution of final products was still unclear. Therefore, 10 % PACE gel was used to separate oligosaccharides with various DPs. As shown in Fig. 3, xylan and longer xylooligosaccharides appeared as a smear at the upper side of the gels, while several peaks appeared after hydrolysis. *PcXyn10A* degraded acetylated xylan mainly into xylooligosaccharides with DP < 10, which is consistent with the value estimated from reducing-sugar analysis. After deacetylation, as expected, *PcXyn10A* xylanases produced smaller oligosaccharides, again in agreement with the biochemical results.

In contrast to *PcXyn10A*, *PcXyn11B* degraded acetylated xylan mainly into large compounds which remained at the upper part of the gel, suggesting that the action of *PcXyn11B* is clearly blocked by acetyl group substitution. However, after deacetylation, *PcXyn11B* produced smaller oligosaccharides and the final products of deacetylated xylan had a DP of 6 or less (Fig. 3B). Although more data is needed to identify final products completely, it was confirmed that acetylated xylan from *A. thaliana* is not a favorable substrate for *PcXyn11B*, in contrast to *PcXyn10A*.

Comparison of degradation of various xylans.

To compare the degradation of various native xylans by

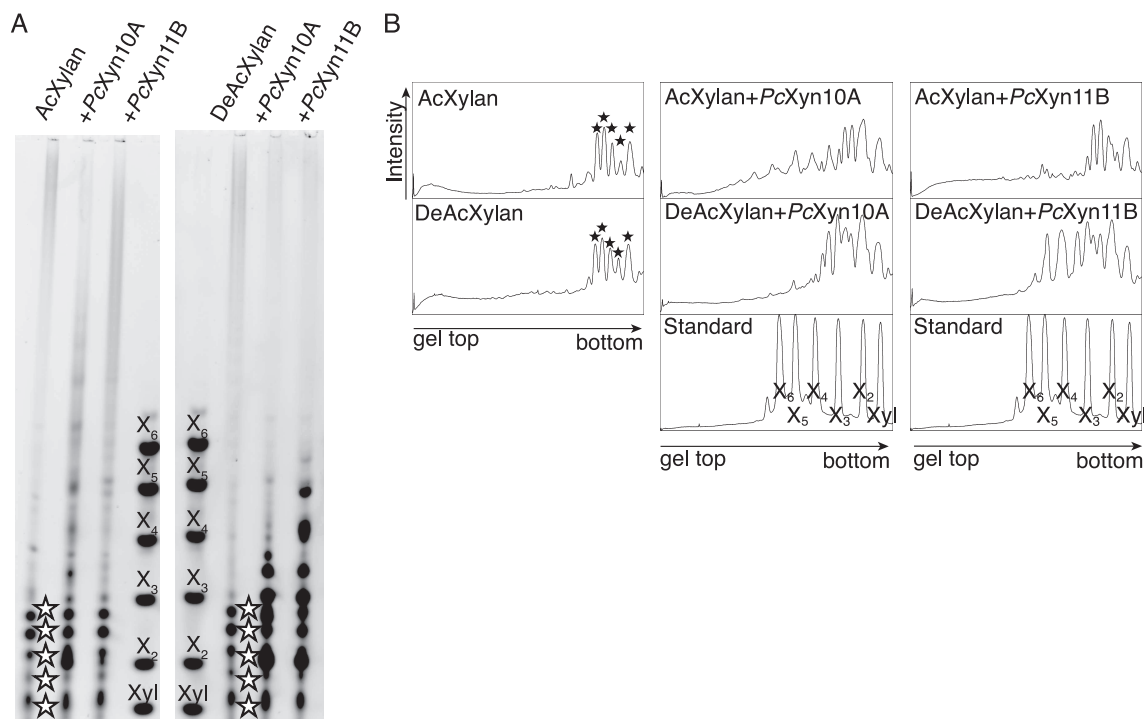


Fig. 3. Effect of acetyl groups on degradation of the xylan main chain.

A: Separation of oligosaccharides using 10 % PACE gel. The components of the reaction solution were the same as for Fig. 2. The reaction was conducted at 30 °C for 24 h. Electrophoresis was run at 1,000 V for 45 min. AcXylan and DeAcXylan mean acetylated xylan from *A. thaliana* and deacetylated xylan after alkali treatment. Xyl, X₂, X₃, X₄, X₅, and X₆ are standard xylooligosaccharides: xylose, xylobiose, xylotriose, xyloetraose, xylopentaose, and xylohexaose, respectively. Stars indicate background bands from substrates. B: Intensity profiles of PACE gels in A analyzed by Image J.

PcXyn10A and *PcXyn11B*, we focused on two acetylated xylans from birch wood and rice straw and one non-acetylated xylan from Japanese cedar. As summarized in Table 1, acetylated xylan from birch wood consisted of 45.5 ± 1.2 % free xylose residues, 51.1 ± 0.8 % acetylated xylose residues and 6.6 ± 0.9 % GlcA-substituted xylose residues. While the acetylation ratio is similar to that of acetylated xylan from *A. thaliana*,⁶⁾ the ratio of GlcA/Xyl is slightly smaller.³⁴⁾ Acetylated xylan from rice straw consisted of 64.5 ± 0.7 % free xylose residues, 25.9 ± 0.8 % acetylated xylose residues, 0.8 ± 0.1 % GlcA-substituted xylose residues and 8.7 ± 0.3 % Araf-substituted xylose residues. It has been reported that acetylated xylans from grasses contain 60–80 % free xylose residues, while other xylose residues are substituted mostly with acetyl groups, as well as Araf and GlcA in that order.⁷⁾ Non-acetylated xylan from Japanese cedar consisted of 74.8 ± 0.4 % free xylose residues, 17.4 ± 0.2 % GlcA-substituted xylose residues and 7.8 ± 0.6 % Araf-substituted xylose residues. The ratios of GlcA/Xyl and Araf/Xyl are approximately 1/6 and 1/13, respectively. Two major motifs of non-acetylated xylan from softwood were previously identified as α -L-arabinofuranosyl- α -D-glucuronyl xylohexaose and α -D-glucuronyl xylohexaose,⁴¹⁾ and small amounts of other motifs are also present.⁴²⁾ These values are similar to those of non-acetylated xylan from softwoods.

The results of digestion of the three selected xylans by *PcXyn10A* and *PcXyn11B* are shown in Fig. 4. *PcXyn10A* degraded acetylated xylan from birch wood similarly to acetylated xylan from *A. thaliana*. The pattern of degradation products of acetylated xylan from rice straw was similar to that of acetylated xylan from birch wood (Fig. 4A), whereas their components are different. *PcXyn10A* produced

smaller oligosaccharides from acetylated xylan of rice straw as compared with those from acetylated xylan of birch wood due to less acetylation of rice straw xylan. The peak intensities were quantified by Image J as shown in Fig. 4B. The final products of acetylated xylans from both plants were mainly oligosaccharides with DP < 15, as in the case of *A. thaliana*. The results for *PcXyn11B* are also shown in Fig. 4. *PcXyn11B* did not degraded acetylated xylans as well as *PcXyn10A*, as was the case for the acetyl xylan from *A. thaliana*. However, non-acetylated xylan from Japanese cedar was degraded well not only by *PcXyn10A*, but also by *PcXyn11B*. These results are consistent with the idea that acetyl group substitution can interfere with the action of GH11 enzymes, but not GH10 enzymes much.

The evolutionary relationship between fungal xylanases and AXEs.

Figure 5 shows the putative relationship between fungal evolution and the numbers of GH10, GH11 xylanases and CE1 enzymes which are classified as AXEs,⁶⁾ based on previous research.³⁵⁾ To examine the relationships of these enzymes in fungal xylan degradation systems, the correlation coefficients between the numbers of enzymes were calculated (Table 3). The correlation between numbers of GH10 and GH11 enzymes is weak (correlation coefficient less than 0.5), while numbers of CE1 enzymes show high correlation coefficients of approximately 0.7 with the numbers of both GH10 and GH11 enzymes. These results suggest that fungi possessing a large number of xylanases also tend to possess a large number of AXEs.

Furthermore, the correlation coefficient between the existence of GH10 and CE1 enzymes is low, under 0.4,

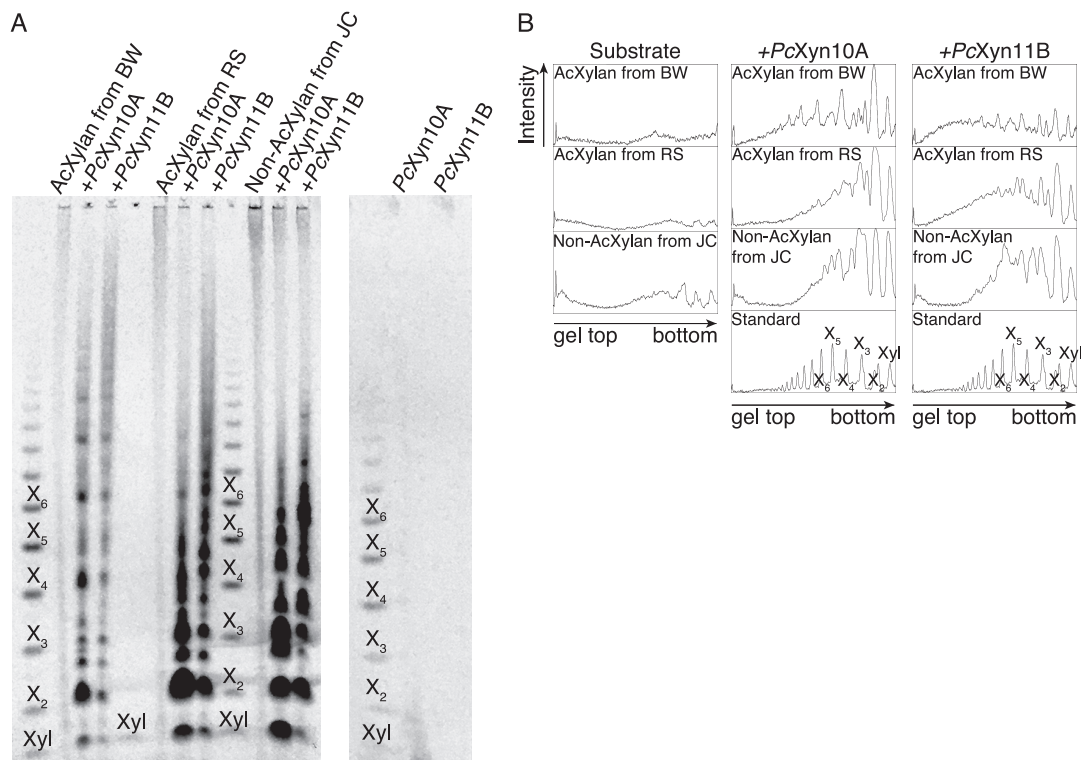


Fig. 4. Comparison of native xylan degradation properties by PACE.

A: Comparison of the degradation of various xylans using 10 % PACE gels. AcXylan from BW, AcXylan from RS, Non-AcXylan from JC indicate acetylated xylan from birch wood, acetylated xylan from rice straw, and non-acetylated xylan from Japanese cedar. Electrophoresis was run at 1,000 V for 1 h. Acetylated xylans from birch wood and rice straw were extracted by DMSO after delignification. Non-acetylated xylan from Japanese cedar was extracted using 4 M KOH. B: Analysis of gel bands by Image J. The X axis represents the location in the gel and the Y axis represents the intensity of each band.

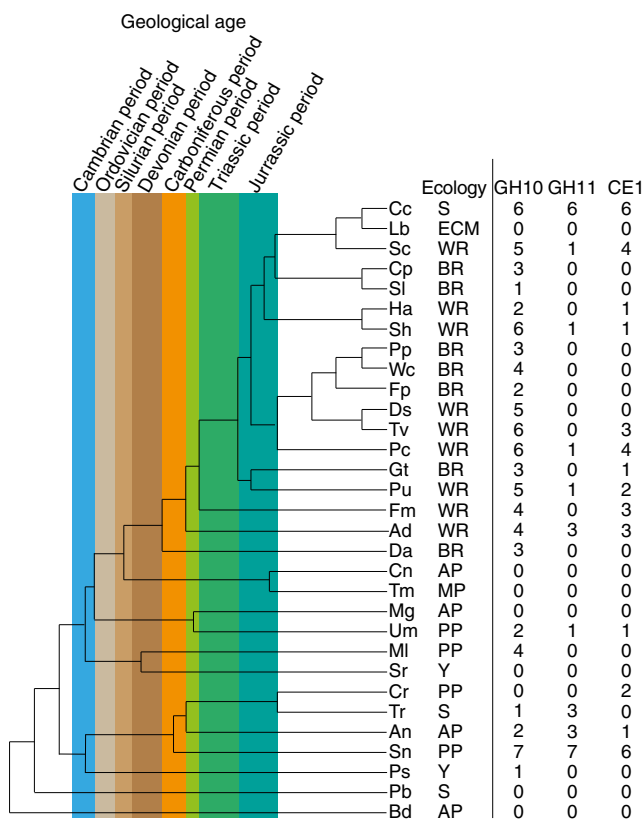


Fig. 5. Fungal phylogenetic tree with the numbers of GH10, GH11, and CE1 enzymes.

The fungal phylogenetic tree and the numbers of enzymes are based on a previous report.³⁵ S, ECM, WR, BR, AP, MP, PP, and Y in the Ecology column mean non-wood decaying saprotroph, mycorrhiza, white-rot, brown-rot, animal pathogen/parasite, mycoparasite, plant pathogen, and yeast, respectively. Refer to the previous paper³⁵ for fungal names.

Table 3. The correlation coefficients between the numbers (left, bottom) and the existence (right upper) of GH10, GH11, and CE1 enzymes.

	GH10	GH11	CE1
GH10			
GH11	0.47		
CE1	0.69	0.72	

Data on the numbers and the existence of GH10, GH11, and CE1 enzymes were taken from Floudas *et al.*³⁵

while that between the existence of GH11 and CE1 enzymes is approximately 0.6. Nine of 10 fungi having GH11 xylanase genes have CE1 genes, though only 14 fungi carry CE1 genes among the 31 fungi considered here. These results suggest that coevolution of these families' enzymes may have occurred. This seems plausible because GH11 enzymes would require deacetylation by CE1 AXEs in order to work well in hydrolyzing xylan.

It is worth noting that acetyl group(s) should be removed even after degradation by GH10 enzymes in order to facilitate the reaction of glycosidases. Thus, there may be so-far-unidentified AXEs associated with GH10. In evolutionary terms, it seems that GH10 xylanases appeared much earlier than GH11 xylanases, and fungi and molds may have acquired GH11 and CE1 concomitantly from the Carboniferous period to the Permian period, when gymnosperms and angiosperms appeared. Brown-rot fungi tend to have fewer GH11 and CE1 enzymes in their genome, which is reasonable because these fungi prefer softwood to hardwood. Thus, the evolution of plant species having acetyl side chains on

xylan may have led to the appearance of relevant enzymes in fungal xylan-degrading systems.

We believe the present findings will be helpful not only in understanding how plant biomass is degraded in nature, but also in improving the efficiency of human utilization of cellulosic biomass.

CONFLICTS OF INTEREST

The authors declare no conflict of interests.

ACKNOWLEDGMENTS

We wish to thank Professor Harry Gilbert for the kind gift of CjGH10. This work was supported in part by a Grant-in-Aid for Scientific Research (B) 19H03013 (to K.I.), a Grant-in-Aid for Early-Career Scientists 19K15884 (to N.S.) from the Japan Society for the Promotion of Science (JSPS), a Grant-in-Aid for Innovative Areas 18H05494 (to K.I.) from the Japanese Ministry of Education, Culture, Sports, and Technology (MEXT) and Environment Research and Technology Development Fund No. JPMEERF21S11900 and JPMEERF21S11902 (to K.I.) from the Environmental Restoration and Conservation Agency of Japan (ERCA).

REFERENCES

- 1) K. Sakuragi, K. Igarashi, and M. Samejima: Application of ammonia pretreatment to enable enzymatic hydrolysis of hardwood biomass. *Polym. Degrad. Stab.*, **148**, 19–25 (2018).
- 2) T.J. Simmons, J.C. Mortimer, O.D. Bernardinelli, A.C. Pöppler, S.P. Brown, E.R. DeAzevedo, R. Dupree, and P. Dupree: Folding of xylan onto cellulose fibrils in plant cell walls revealed by solid-state NMR. *Nat. Commun.*, **7**, 1–9 (2016).
- 3) T. Wang, H. Yang, J.D. Kubicki, and M. Hong: Cellulose structural polymorphism in plant primary cell walls investigated by high-field 2D solid-state NMR spectroscopy and density functional theory calculations. *Biomacromolecules*, **17**, 2210–2222 (2016).
- 4) N. Takahashi and T. Koshijima: Ester linkages between lignin and glucuronoxylan in a lignin-carbohydrate complex from beech (*Fagus crenata*) wood. *Wood Sci. Technol.*, **22**, 231–241 (1988).
- 5) X. Du, M. Pérez-Boada, C. Fernández, J. Rencoret, J.C. del Río, J. Jiménez-Barbero, J. Li, A. Gutiérrez, and A.T. Martínez: Analysis of lignin-carbohydrate and lignin–lignin linkages after hydrolase treatment of xylan-lignin, glucmannan-lignin and glucan-lignin complexes from spruce wood. *Planta*, **239**, 1079–1090 (2014).
- 6) M. Busse-Wicher, T.C.F. Gomes, T. Tryfona, N. Nikolovski, K. Stott, N.J. Grantham, D.N. Bolam, M.S. Skaf, and P. Dupree: The pattern of xylan acetylation suggests xylan may interact with cellulose microfibrils as a twofold helical screw in the secondary plant cell wall of *Arabidopsis thaliana*. *Plant J.*, **79**, 492–506 (2014).
- 7) D. Morais de Carvalho, A.M. Abad, D.V. Evtuguin, J.L. Colodette, M.E. Lindström, F. Vilaplana, and O. Sevastyanova: Isolation and characterization of acetylated glucuronarabinoxylan from sugarcane bagasse and straw. *Carbohydr. Polym.*, **156**, 223–234 (2017).
- 8) P. Biely, S. Singh, and V. Puchart: Towards enzymatic breakdown of complex plant xylan structures: state of the art. *Biotechnol. Adv.*, **34**, 1260–1274 (2016).
- 9) P. Biely, M. Cziszárová, I. Uhliariková, J.W. Agger, X.L. Li, V.G.H. Eijsink, and B. Westereng: Mode of action of acetylxylan esterases on acetyl glucuronoxylan and acetylated oligosaccharides generated by a GH10 endoxylanase. *Biochim. Biophys. Acta-Gen. Subj.*, **1830**, 5075–5086 (2013).
- 10) V. Lombard, H. Golaconda Ramulu, E. Drula, P.M. Coutinho, and B. Henrissat: The carbohydrate-active enzymes database (CAZy) in 2013. *Nucleic Acids Res.*, **42**, 490–495 (2014).
- 11) C. Hori, J. Gaskell, K. Igarashi, M. Samejima, D. Hibbett, B. Henrissat, and D. Cullen: Genomewide analysis of polysaccharides degrading enzymes in 11 white- and brown-rot Polyporales provides insight into mechanisms of wood decay. *Mycologia*, **105**, 1412–1427 (2013).
- 12) P. Biely, M. Vršanská, M. Tenkanen, and D. Kluepfel: Endo- β -1,4-xylanase families: differences in catalytic properties. *J. Biotechnol.*, **57**, 151–166 (1997).
- 13) G. Pell, E.J. Taylor, T.M. Gloster, J.P. Turkenburg, C.M.G.A. Fontes, L.M.A. Ferreira, T. Nagy, S.J. Clark, G.J. Davies, and H.J. Gilbert: The mechanisms by which family 10 glycoside hydrolases bind decorated substrates. *J. Biol. Chem.*, **279**, 9597–9605 (2004).
- 14) Z. Fujimoto, S. Kaneko, A. Kuno, H. Kobayashi, I. Kusakabe, and H. Mizuno: Crystal structures of decorated xylooligosaccharides bound to a family 10 xylanase from *Streptomyces olivaceoviridis* E-86. *J. Biol. Chem.*, **279**, 9606–9614 (2004).
- 15) M. Vardakou, C. Dumon, J.W. Murray, P. Christakopoulos, D.P. Weiner, N. Juge, R.J. Lewis, H.J. Gilbert, and J.E. Flint: Understanding the structural basis for substrate and inhibitor recognition in Eukaryotic GH11 xylanases. *J. Mol. Biol.*, **375**, 1293–1305 (2008).
- 16) Z. Fujimoto, N. Kishine, K. Teramoto, S. Tsutsui, and S. Kaneko: Structure-based substrate specificity analysis of GH11 xylanase from *Streptomyces olivaceoviridis* E-86. *Appl. Microbiol. Biotechnol.*, **105**, 1943–1952 (2021).
- 17) D. Martinez, L.F. Larrondo, N. Putnam, M.D. Sollewijn Gelpke, K. Huang, J. Chapman, K.G. Helfenbein, P. Ramaiya, J.C. Detter, F. Larimer, P.M. Coutinho, B. Henrissat, R. Berka, D. Cullen, and D. Rokhsar: Genome sequence of the lignocellulose degrading fungus *Phanerochaete chrysosporium* strain RP78. *Nat. Biotechnol.*, **22**, 695–700 (2004).
- 18) S.M. Kremer and P.M. Wood: Evidence that cellobiose oxidase from *Phanerochaete chrysosporium* is primarily an Fe(III) reductase: kinetic comparison with neutrophil NADPH oxidase and yeast flavocytochrome *b₂*. *Eur. J. Biochem.*, **205**, 133–138 (1992).
- 19) J.J. Almagro Armenteros, K.D. Tsirigos, C.K. Sønderby, T.N. Petersen, O. Winther, S. Brunak, G. von Heijne, and H. Nielsen: SignalP 5.0 improves signal peptide predictions using deep neural networks. *Nat. Biotechnol.*, **37**, 420–423 (2019).
- 20) R. Dustin Schaeffer, Y. Liao, H. Cheng, and N.V. Grishin: ECOD: New developments in the evolutionary classification of domains. *Nucleic Acids Res.*, **45**, D296–D302 (2017).
- 21) K. Igarashi, T. Ishida, C. Hori, and M. Samejima: Character-

- ization of an endoglucanase belonging to a new subfamily of glycoside hydrolase family 45 of the basidiomycete *Phanerochaete chrysosporium*. *Appl. Environ. Microbiol.*, **74**, 5628–5634 (2008).
- 22) K. Igarashi, M. Maruyama, A. Nakamura, T. Ishida, M. Wada, and M. Samejima: Degradation of crystalline celluloses by *Phanerochaete chrysosporium* cellobiohydrolase II (Cel6A) heterologously expressed in methylotrophic yeast *Pichia pastoris*. *J. Appl. Glycosci.*, **59**, 105–110 (2012).
- 23) R.T. DeBoy, E.F. Mongodin, D.E. Fouts, L.E. Tailford, H. Khouri, J.B. Emerson, Y. Mohamoud, K. Watkins, B. Henrissat, H.J. Gilbert, and K.E. Nelson: Insights into plant cell wall degradation from the genome sequence of the soil bacterium *Cellvibrio japonicus*. *J. Bacteriol.*, **190**, 5455–5463 (2008).
- 24) F. Goubet, C. J. Barton, J. C. Mortimer, X. Yu, Z. Zhang, G. P. Miles, J. Richens, A.H. Liepman, K. Seffen, and P. Dupree: Cell wall glucomannan in *Arabidopsis* is synthesised by CSLA glycosyltransferases, and influences the progression of embryogenesis. *Plant J.*, **60**, 527–538 (2009).
- 25) W. Klauz: Zur biologisch-mechanischen wirkung der cellulose und hemicellulose im festigungsgewebe der Laubhölzer. *Holzforschung*, **11**, 110–116 (1957).
- 26) T. Awano, K. Takabe, and M. Fujita: Xylan deposition on secondary wall of *Fagus crenata* fiber. *Protoplasma*, **219**, 106–115 (2002).
- 27) A. Telemán, J. Lundqvist, F. Tjerneld, H. Stålbrand, and O. Dahlman: Characterization of acetylated 4-*O*-methylglucuronoxylan isolated from aspen employing ¹H and ¹³C NMR spectroscopy. *Carbohydr. Res.*, **329**, 807–815 (2000).
- 28) D.V. Evtuguin, J.L. Tomás, A.M.S. Silva, and C.P. Neto: Characterization of an acetylated heteroxylan from *Eucalyptus globulus* Labill. *Carbohydr. Res.*, **338**, 597–604 (2003).
- 29) I. Uhliariková, M. Vršanská, B.V. McCleary, and P. Biely: Positional specificity of acetylxylan esterases on natural polysaccharide: an NMR study. *Biochim. Biophys. Acta - Gen. Subj.*, **1830**, 3365–3372 (2013).
- 30) R. Naran, S. Black, S.R. Decker, and P. Azadi: Extraction and characterization of native heteroxylans from delignified corn stover and aspen. *Cellulose*, **16**, 661–675 (2009).
- 31) P. Naidjonoka, M.A. Hernandez, G.K. Pålsson, F. Heinrich, H. Stålbrand, and T. Nylander: On the interaction of softwood hemicellulose with cellulose surfaces in relation to molecular structure and physicochemical properties of hemicellulose. *Soft Matter*, **16**, 7063–7076 (2020).
- 32) S. Waffenschmidt and L. Jaenicke: Assay of reducing sugars in the nanomole range with 2,2'-bicinchoninate. *Anal. Biochem.*, **165**, 337–340 (1987).
- 33) F. Goubet, P. Jackson, M.J. Deery, and P. Dupree: Polysaccharide analysis using carbohydrate gel electrophoresis. A method to study plant cell wall polysaccharides and polysaccharide hydrolases. *Anal. Biochem.*, **300**, 53–68 (2002).
- 34) J.R. Bromley, M. Busse-Wicher, T. Tryfona, J.C. Mortimer, Z. Zhang, D.M. Brown, and P. Dupree: GUX1 and GUX2 glucuronyltransferases decorate distinct domains of glucuronoxylan with different substitution patterns. *Plant J.*, **74**, 423–434 (2013).
- 35) D. Floudas, M. Binder, R. Riley, K. Barry, R.A. Blanchette, B. Henrissat, A.T. Martínez, R. Otillar, J.W. Spatafora, J.S. Yadav, A. Aerts, I. Benoit, A. Boyd, A. Carlson, A. Copeland, P.M. Coutinho, R.P. De Vries, P. Ferreira, K. Findley, *et al.*: The paleozoic origin of enzymatic lignin decomposition reconstructed from 31 fungal genomes. *Science*, **336**, 1715–1719 (2012).
- 36) S.C. Potter, A. Luciani, S.R. Eddy, Y. Park, R. Lopez, and R.D. Finn: HMMER web server: 2018 update. *Nucleic Acids Res.*, **46**, W200–W204 (2018).
- 37) C. Hori, K. Igarashi, A. Katayama, and M. Samejima: Effects of xylan and starch on secretome of the basidiomycete *Phanerochaete chrysosporium* grown on cellulose. *FEMS Microbiol. Lett.*, **321**, 14–23 (2011).
- 38) K. Sakuragi, C. Hori, K. Igarashi, and M. Samejima: Secretome analysis of the basidiomycete *Phanerochaete chrysosporium* grown on ammonia-treated lignocellulosic biomass from birch wood. *J. Wood Sci.*, **64**, 845–853 (2018).
- 39) M.H. Johansson and O. Samuelson: Alkaline destruction of birch xylan in the light of recent investigations of its structure. *Sven. Papperstidn.*, **80**, 519–524 (1977).
- 40) P. Biely, C.R. Mackenzie, J. Puls, and H. Schneider: Cooperativity of esterases and xylanases in the enzymatic degradation of acetyl xylan. *Nat. Biotechnol.*, **4**, 731–733 (1986).
- 41) M. Busse-Wicher, A. Li, R.L. Silveira, C.S. Pereira, T. Tryfona, T.C.F. Gomes, M.S. Skaf, and P. Dupree: Evolution of xylan substitution patterns in gymnosperms and angiosperms: Implications for xylan interaction with cellulose. *Plant Physiol.*, **171**, 2418–2431 (2016).
- 42) A. Martínez-Abad, J. Berglund, G. Toriz, P. Gatenholm, G. Henriksson, M. Lindström, J. Wohler, and F. Vilaplana: Regular motifs in xylan modulate molecular flexibility and interactions with cellulose surfaces. *Plant Physiol.*, **175**, 1579–1592 (2017).